AGU PUBLICATIONS

Geophysical Research Letters

RESEARCH LETTER
10.1002/2015GL063721

Key Points:
- How does the seismicity behave prior to a major earthquake?
- How a major earthquake affects the seismic activity in regional scale?
- What is the present state of the seismicity in NW Turkey?

Correspondence to:
F. Bulut,
fatihbulut@aydin.edu.tr

Citation:
Bulut, F. (2015), Different phases of the earthquake cycle captured by seismicity along the North Anatolian Fault, *Geophys. Res. Lett.*, *42*, 2219–2227, doi:10.1002/2015GL063721.

Received 3 MAR 2015
Accepted 5 MAR 2015
Accepted article online 11 MAR 2015
Published online 11 APR 2015

Different phases of the earthquake cycle captured by seismicity along the North Anatolian Fault

Fatih Bulut[1]

[1]AFAM Disaster Research Center, Istanbul Aydın University, Istanbul, Turkey

Abstract The North Anatolian Fault has accommodated three major earthquakes during the last 15 years. Although the fault zone has substantially failed during the last century, it did not completely fail in NW Turkey and therefore left several segments at different physical stages. In this study, the seismicity rate is used as a proxy to locate the brittle fault sections with high/low strain accumulation. The results show that the 1999 *M*7.4 İzmit and the 2014 *M*6.9 Aegean earthquakes were preceded by almost a decade-long period of enhanced microearthquake activity representing a brittle process preparing the failure. This interpretation is supported by observed lateral migration of microearthquakes toward the main shock hypocenter within a time scale of roughly a decade. The Sea of Marmara segments of the North Anatolian Fault show a rather temporally uniform seismicity trend leading to the hypothesis that those segments are still not in the preparation stage for a large earthquake. The results also show that the duration of aftershock activity is not controlled only by the size of main shocks.

1. Introduction

The seismic cycle along a shear zone involves the repetitive process of strain accumulation and subsequent release in earthquakes, as is well exemplified by historic earthquakes along the San Andreas Fault (SAF) and the North Anatolian Fault (NAF). The duration of the cycle is controlled by the annual amount of strain accumulation and the strength of the structures resisting failure [e.g., *Lapusta and Rice*, 2003]. Structural relations, fault maturity, and consequent fault strength might vary strongly along a broad shear zone (e.g., NAF [*Şengör et al.,* 2005]). A net result can be irregular periods of failure for individual fault segments. A second factor is variations in strain rates. As the whole system is connected via an elastic upper crust, failure of a segment might increase or decrease strain rates advancing or retarding upcoming failure on a neighboring segment [*King et al.,* 1994].

In practice, there are only a few examples on the Earth where all stages of the earthquake cycle have been properly monitored seismically and geodetically (e.g., entire cycle at Parkfield segment of the SAF in California, USA [*Segall and Harris*, 1987], and preseismic, coseismic, and postseismic periods for the Izmit segment of the NAF [*Bürgmann et al.,* 2002]). In this study, two earthquakes along the NAF in NW Turkey and the Aegean are selected to investigate seismicity patterns at different phases of the earthquake cycle.

The basic elements of the tectonic framework in Turkey and its immediate surroundings are extension in the Aegean region in the west, continental convergence between the Arabian and Eurasian plates in the east, and the westward movement of the Anatolian Plate in the middle [*Jackson and McKenzie*, 1988; *Taymaz et al.,* 1990, 1991; *Yolsal-Çevikbilen and Taymaz*, 2012] (Figure 1, inset). Westward motion of the Anatolian region results in strain accumulation along the plate-bounding transform fault zones, the NAF and the East Anatolian Fault (EAF) (Figure 1, inset). Presently, the NAF accommodates right-lateral strike-slip rates ranging between 23 and 28 mm/yr while the EAF accommodates left-lateral strike-slip rates of ~9 mm [*Reilinger et al.,* 2006].

The NAF acts as a transform plate boundary between the Eurasian and Anatolian plates extending for ~1200 km along northern Turkey starting from the Bingöl-Karlıova triple junction and extending to the Northern Aegean Sea [*Şengör and Yılmaz,* 1981]. The main branch of the fault failed during the last century in a westward migrating pattern of large earthquakes [*Toksöz et al.,* 1979]. The twentieth century sequence initiated with a $M = 7.4$ earthquake on the Ganos segment west of the Sea of Marmara but then jumped to the eastern end of the fault with the Erzincan, 1939 (M 7.9) event. Subsequent large events more or less systematically ruptured the fault zone toward the west up to the İzmit-Düzce segment where the 1999 M 7.4 and M 7.1 earthquakes ruptured about 180 km section of the NAF. The 1999 earthquake ruptures represent

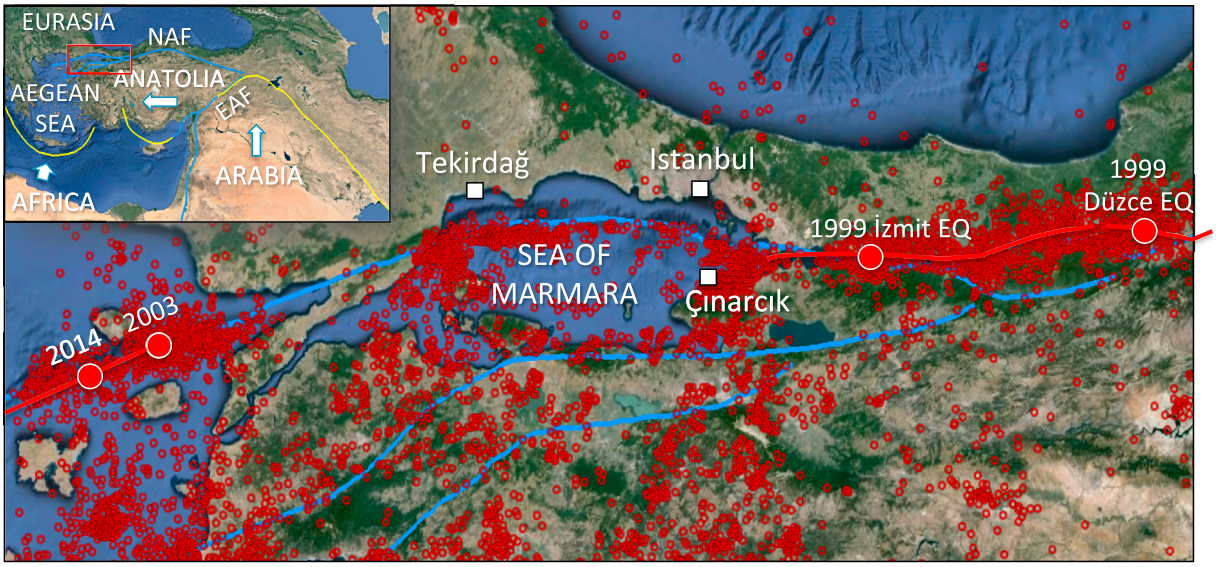

Figure 1. Introduction to seismicity and seismotectonics in NW Turkey. The target area accommodated three major earthquakes during time period of my analysis. These are the 1999 İzmit (M 7.4), the 1999 Düzce (M 7.2), and the 2014 Aegean (M 6.9) earthquakes (large red dots). Red lines show the rupture zones, and blue lines indicate North Anatolian Fault (NAF) segments. Red circles are the earthquake epicenters ($M > 3.0$) for the time period 1990–2014. (inset) The basic tectonic elements in the Anatolian region and its surroundings. Red frame shows the target area.

the present western end of this migrating sequence. However, the migration jumped to the Northern Aegean Sea in a further westward advance during the 2014, M 6.9 Aegean earthquake (Figure 1) [*Evangelidis*, 2015].

The segments remaining between the 1999 İzmit-Düzce and the 2014 Aegean earthquakes are considered to be a seismic gap, not having completed the last seismic cycle along the NAF. In this context, the seismicity in NW Turkey is analyzed to provide insights into stochastic interaction of the seismicity along the NAF segments in the Sea of Marmara region and surrounding fault segments. The sensitivity of the earthquake catalog used is elaborated in time and space, and spatiotemporal variation of the number of events, as well as seismic moment release, is investigated before and after the large earthquakes in the target area. Seismicity zones are further analyzed to understand the brittle deformation prior to and following the major earthquakes and to provide insights into earthquake forecasting and hazard assessment.

2. Earthquake Catalog

Kandilli Observatory and Earthquake Research Institute (KOERI) has been continuously monitoring earthquake activity in Turkey since 1934. Technological and economical developments allowed improving the earthquake monitoring conditions during recent decades. Therefore, the magnitude of completeness (M_c) in NW Turkey has been lowered to ~M 2.5. This provides a broad data set to investigate the seismicity along the NAF in NW Turkey.

The target area is presently being monitored by KOERI using 46 seismic stations. The station spacing ranges between 20 and 70 km resulting in detection of a total of 21,721 earthquakes in NW Turkey since 1990. However, the catalog is restricted to the M_c of 3.0, which is found to be the highest M_c for the target area. This lowered the number of earthquakes analyzed down to 4050 for the time period of 1990–2014. The location uncertainty reaches up to 5 km, and the grid size used in this analysis is fixed at 10 km, as the intention is to focus on regional-scale features (KOERI) [*Kalafat et al.,* 2008].

M_c is calculated using cumulative frequency of magnitudes. The break in slope of frequency versus magnitude determines M_c for a given data set [*Gutenberg and Richter*, 1954]. This calculation is performed for subsets in time and space to investigate spatiotemporal variation of M_c. Each subset consists of at least 30 events to ensure the statistical basis. Magnitudes are converted to seismic moment (M_0) using the relation

$$M_w = \frac{2}{3}\log_{10}(M_0) - 6.0$$

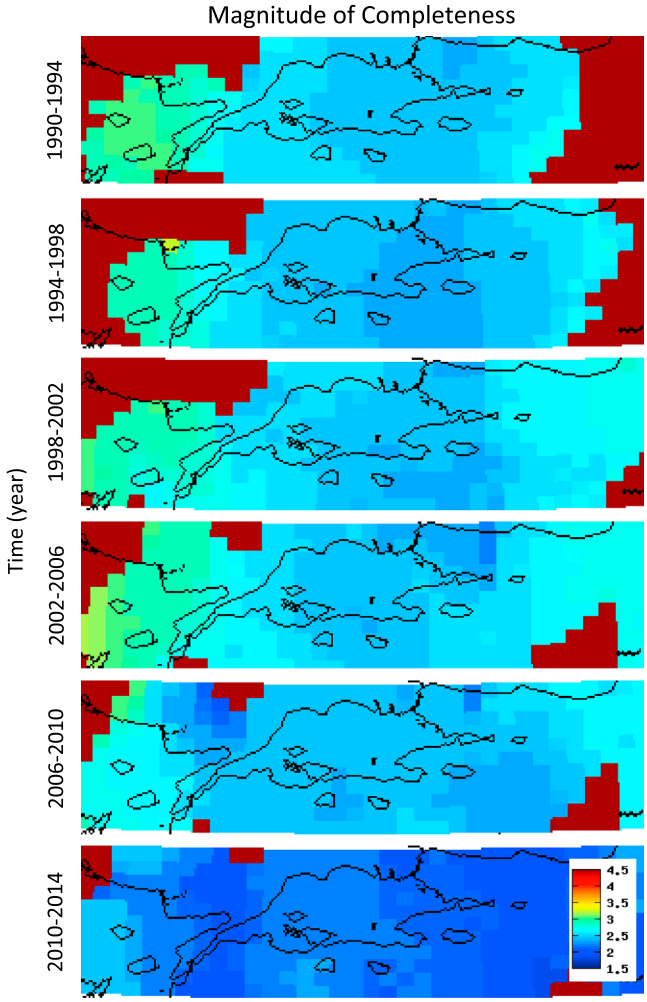

Figure 2. Temporal variation of earthquake detection threshold in NW Turkey based on magnitude of completeness (M_c). The data set is split into the time slices of 4 years.

where M_w represents the earthquake magnitudes in the catalog and M_0 is the seismic moment [*Hanks and Kanamori*, 1979]. Cumulative seismic moments as well as number of earthquakes are mapped to capture locations with prominent seismicity clusters. Those spots are investigated also in the time domain to give insights into the spatiotemporal behavior of the seismicity.

3. Results

3.1. Sensitivity of Seismic Network

The monitoring capacity of the National Seismic Network in NW Turkey has been significantly improved during recent decades. Therefore, I investigate the temporal and spatial variations in M_c to quantify the sensitivity of the seismic network in the target area. In this context, the distribution of M_c is divided into 4 year time slices (Figure 2). For the time period of 1990–2010, the M_c remains almost unchanged, ranging from ~*M*2.5 to *M* ~ 3.0 except for several outliers outside the primary deformation zone of the NAF. The spatial distribution of M_c, highest (~*M*3.0) in the west and lower toward the eastern Sea of Marmara region, is due to the denser seismic network in the vicinity of Istanbul. M_c was significantly improved starting in 2010, to ~*M* 2.5 for the entire NW Turkey region. Based on the high variation of M_c and therefore unstable detection threshold in time and space, the earthquake catalog is restricted to events above *M* 3.0, the highest M_c for the entire region and time period of my analysis.

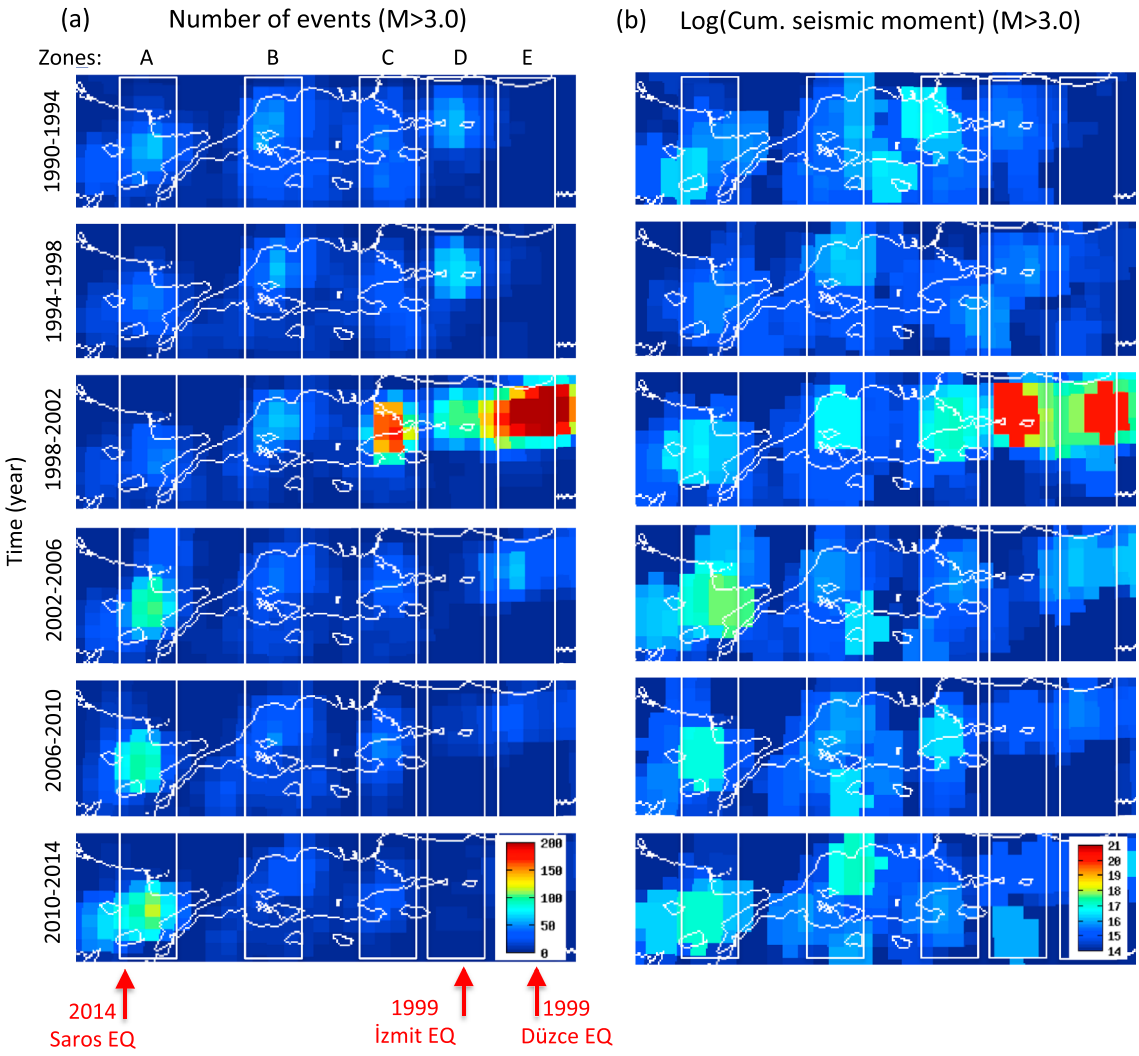

Figure 3. Spatiotemporal evolution of the seismicity in NW Turkey between 1990 and 2014 based on (a) number of events and (b) seismic moment. The data set is restricted to the earthquake magnitudes larger than 3.0 and split into the time slices of 4 years.

3.2. Long-Lasting Earthquake Clusters

After filtering out earthquakes below the highest M_c for the entire target region, I investigate the spatial distribution of the number of events and the cumulative seismic moment release for time windows of 4 years for the time period 1990–2014. My main motivation is to identify regions with high seismic activity. The map view of the number of events reflects five zones along the northern segments of the North Anatolian Fault in NW Turkey (zones A–E, Figure 3a).

Zone A is located in Northern Aegean Sea, in close proximity to the nucleation area of the 2014 Aegean earthquake (*M* 6.9). This area always hosts a high number of earthquakes for the entire time period of our analysis and furthermore reflects a drastic acceleration starting during the time frame of 2002–2006, when the number of events has almost doubled compared to the seismicity rate in the past (Figure 3a). Similarly, cumulative seismic moment increases while the change is not as drastic as seen in the number of earthquakes (Figure 3b).

Zone B is located in Tekirdağ Basin in the western Sea of Marmara region. This area hosts a high number of earthquakes for the time period 1990–2002. The activity is high between 1990 and 2002 and slightly lower for the time period 2002–2014. However, it still remains high compared to more quiet zones (Figure 3a).

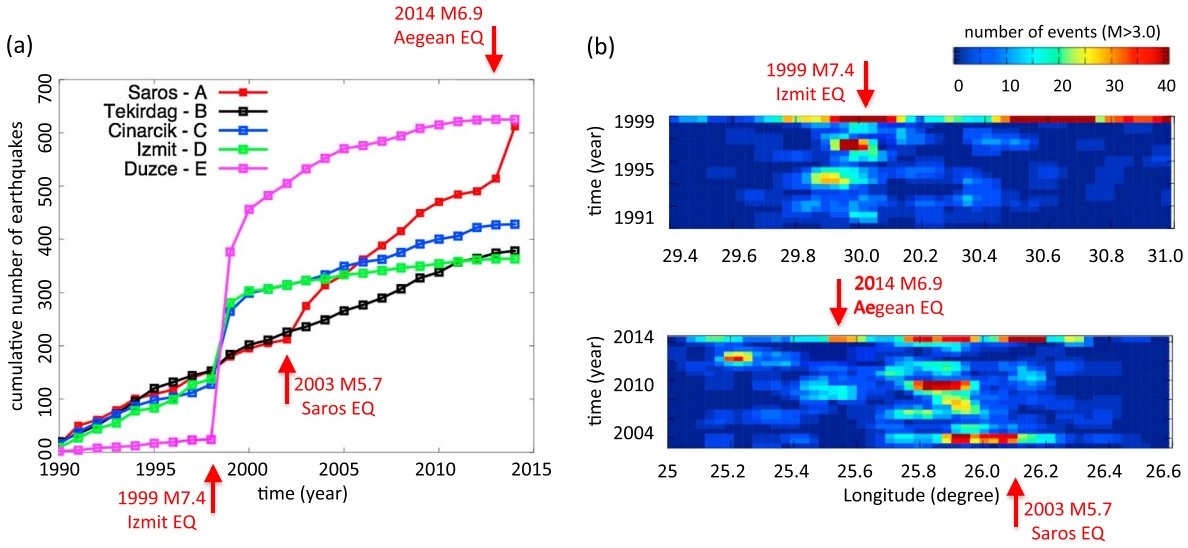

Figure 4. (a) Cumulative number of events ($M > 3.0$) is compared to the time to characterize temporal behavior of identifies seismicity zones, which are extracted from Figure 3a. (b) Preshock activity of the (top) 1999 İzmit and (bottom) 2014 Aegean earthquakes. Arrows show locations of the main shocks, and the color scale shows the number of events above M 3.0.

Clustering here reflects several peaks in cumulative seismic moment corresponding to the main shocks of three $M \geq 5$ earthquakes that took place in 1995, 2002, and 2011 (Figure 3b).

Zone C represents the seismicity in the area of the Çınarcık Basin and its surroundings. This region includes the western section of the 1999 İzmit rupture zone. This region is consistently active for the entire time period of my analysis. However, it reflects a significant peak for the time period 1998–2002, which covers the coseismic and postseismic period of the 1999 İzmit earthquake (Figure 3a). Cumulative seismic moment does not show a stable distribution in time and reflects two other peaks in 1991 and 2008, corresponding to two moderate size earthquakes of M 5.0 and M 4.8, respectively (Figure 3b).

Zone D is located in the nucleation area of the 1999 İzmit earthquake (M 7.4). This area is characterized by a high rate of seismic activity for the time period 1990–2002 that subsequently disappears during the time period 2002–2012. This drastic change occurs around the time of the 1999 İzmit earthquake (Figure 3a). The spatiotemporal distribution of cumulative seismic moment does not show a similar behavior, except for a significant increase during the time period 1998–2002, corresponding to the 1999 İzmit main shock (Figure 3b).

Zone E is located in the eastern most section of the 1999 İzmit earthquake and also the 1999 Düzce earthquake coseismic fault (M 7.2) that occurred 87 days after the Izmit event. This zone shows minor activity before the 1999 earthquakes. The peak in activity in 1999 lasts until 2010 (Figure 3a). Similarly, cumulative seismic moments show high values in 1999, when both major earthquakes occurred (Figure 3b).

In general, seismic moment plots are dominated by the main shocks or the largest events of the seismicity zone. The cumulative number of events gives a better idea about ongoing brittle deformation. Therefore, the discussion is done based on the results from the analysis of cumulative number of events.

3.3. Seismicity Rates

The cumulative numbers of earthquakes are investigated versus time to give better insight into the temporal behavior of the seismicity in NW Turkey (Figure 4a). This is performed for the five featured zones that are shown in Figure 3. Zones A–D show almost the same trend until the 1999 İzmit and Düzce earthquakes. In the time slot including both main shocks, zones C and D start showing the aftershock response for 2 years while zones A and B remain almost unchanged.

Zone A reflects a dramatic jump following the 2003 Saros earthquake (M 5.7) as well as a significant change in slope suggesting an acceleration in seismicity following the 2003 event and lasting until the 2014 Aegean earthquake that occurred ~50 km farther west on the same fault. Zone B shows a roughly stable trend for the

entire period of my analysis expect for a small kink in 1999. This confirms the pattern seen by 4 year time slices on map views (Figure 3a). Zones A and B do not show a major response to the 1999 İzmit and Düzce earthquakes.

Zone E, located in the focal area of the 1999 Düzce earthquake, shows a completely different pattern from other four zones, same as captured by 4 year time slices (Figure 3a). For the time period of 1990–1999, it hosts a very low rate of seismic activity while in 1999 it shows the largest change in seismicity rate for the entire period of my analysis. A second unusual point is that it took almost 10 years to return to the background seismicity rate while zone D, and therefore the focal area of 1999 İzmit earthquake, shows a faster decrease of postseismic response in its hypocentral area within only 2 years. Finally, zone D shows the lowest seismicity rate compared to the other zones after 2001 (Figure 3a).

4. Discussion

One of the key observations obtained in this study is that the 1999 Izmit and the 2014 Aegean earthquake nucleation areas accommodate long-lasting microearthquake activity. In both cases, the number of microearthquakes is high for ~10 years prior to the forthcoming large earthquakes. Here those long-lasting microearthquake activities are interpreted to represent preseismic brittle deformation preparing the ready-to-fail stage. This fracturing might be due to the physical process at the nucleation areas that lead to the forthcoming earthquake. Understanding the stochastic relation between the preshocks and the main shocks requires a closer look at the seismicity along the 2014 rupture zone. Toward that end, the number of events is plotted versus time and longitude to extract spatiotemporal seismicity features along the relevant fault section (Figure 4b).

In principle, there are two basic parameters that control the failure process: Stress accumulation and friction. Assuming that the stress accumulation continues uniformly, failure occurs as the strength of the fault is exceeded by the accumulated stress. The strength of the fault is a function of friction. Here friction might be due not only to fault roughness but also to fault complexity/internal friction of intact rock, depending on the maturity of fault zone/roughness along the fault plane. The NAF in the NW Turkey is a very young shear zone [*Şengör et al.,* 2005] although it started to develop in the Eastern Turkey ~10 Ma ago [*Şengör et al.,* 2005]. In the west, the fault consists of a broad shear band characterized by strongly varying short fault segments, while it is a mature, single fault in the Eastern Turkey [*Barka*, 1996]. In this context, the segments strongly deviating from the overall trend of the NAF represent high-friction spots along the fault zone and therefore might behave as the most resisting section against the failure. The long-lasting preshock activity seen at the 1999 nucleation area might be interpreted to represent fracturing of such a spot until the internal strength is exceeded by the strain accumulation (Figure 4b). This activity has finalized by the last minute foreshocks before the 1999 İzmit earthquake [*Bouchon et al.,* 2011].

This issue might be addressed using a high-resolution structural image in the near vicinity to the 1999 Izmit main shock. The 1999 Izmit aftershocks have been previously relocated using the Double-Difference method (Figure 5a) [*Bulut and Aktar*, 2007]. The method employs cross-correlation derived differential travel times to improve the relative accuracy of hypocenter locations for colocated event families [*Waldhauser and Ellsworth*, 2000]. The hypocenters allow imaging the structural variation of the NAF within the hypocentral area on a resolved scale of several hundred meters. The main shock occurs very close to a ~10 km long NE-SW trending segment that strongly deviates from the overall E-W oriented strike of the NAF. This observation supports the notion that the 1999 Izmit hypocenter occurred on a complexly segmented section of the NAF rather than a mature single fault. Perhaps the long-lasting preshock activity before the main shock represents the fracturing of high-strength sections in response to ongoing tectonic loading.

How long enhanced seismicity lasted before the Izmit earthquake can be addressed by extending our analysis to longer time periods. Therefore, the Izmit Zone (zone D) is reinvestigated starting from 1965. M_c shows a clear improvement between 1965 and 1975 as it goes down from 4.5 to M 2.5 (Figure 5b, blue line). Starting 1975, M_c reflects a rather stable pattern around M 2.5 except for some minor fluctuations up to ± 0.2 (Figure 5b, blue line). Therefore, I restrict the catalog to earthquakes above M 2.8. The cumulative number of earthquakes is investigated for the stable period starting in 1975 using the restricted earthquake catalog (Figure 5b, green line). This analysis shows a clear transition from a shallow to a steep slope in seismicity rate during the time period of 1985–1990. Following this period, the seismicity reflects a stable, high occurrence rate.

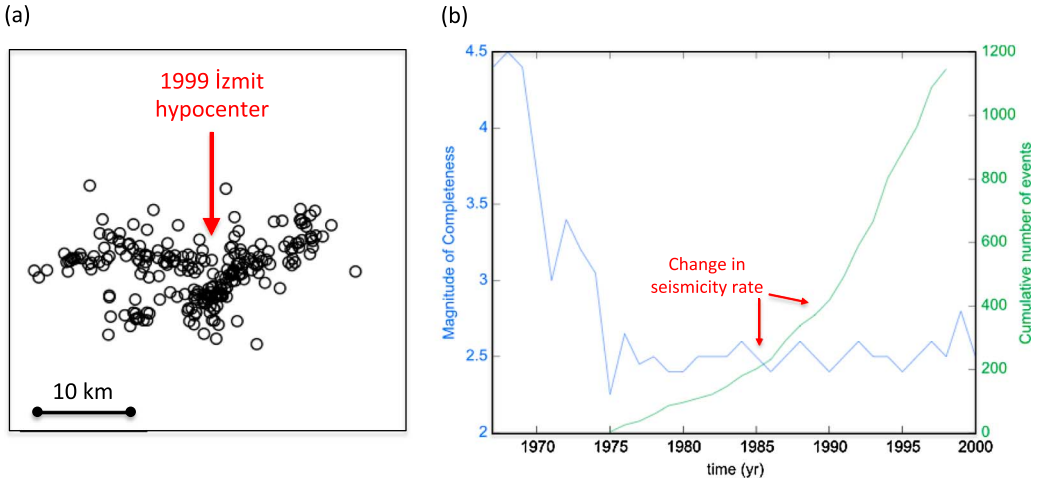

Figure 5. (a) Epicentral distribution of the 1999 Izmit aftershocks in the vicinity of main shock based on precise earthquake locations. (b) Magnitude of completeness as well as cumulative number of events ($M > 2.8$) is compared to the time to characterize temporal behavior of Izmit cluster (zone D).

Interestingly, the seismic activity in the vicinity of the 2014 Aegean earthquake accelerated following the 2003 Saros earthquake (*M* 5.7). The 2003 Saros earthquake involved a westward developing, unilateral rupture process [*Karabulut et al.,* 2006]. The hypocenter of the main shock lies close to the eastern tip of the rupture zone, while the aftershocks are distributed along the entire rupture zone (Figure 4b). Following the aftershock period, the seismicity starts to migrate and expand toward the 2014 rupture zone, consistent with the westward rupture process of the 2003 Saros earthquake. The brittle deformation is accelerated following the 2003 Saros earthquake and expanded to the west within a time period of ~10 years. This large change in seismicity rate suggests a transition from an interseismic to preseismic phase. GPS measurements on the adjacent Ganos segment of the NAF show relatively high-rate lateral deformation compared to the other locations in NW Turkey [*Ergintav et al.,* 2014]. The slip rates on the Ganos and the Northern Aegean segments of the NAF are very similar based on block models [*Meade et al.,* 2002; *Reilinger et al.,* 2006], and therefore, relatively high slip rate on the Ganos segment during the last decade might be extrapolated toward the Northern Aegean segment. I speculate that the observed laterally migrating deformation zone reflects the preparation phase of the 2014 earthquake.

Following the 1999 Izmit earthquake, seismic activity at the hypocentral area drops sharply within 2 years (Figures 3a and 3b, zone D). This is likely due to the fact that the stress concentration at nucleation zone has been released during the failure and redistributed toward the rest of rupture zone. Therefore, the aftershocks are, in general, located outside main shock hypocenter (Figure 3a 1998–2002, zones C and E). However, aftershock activity of the 1999 Düzce earthquake lasts much longer compared to the 1999 Izmit earthquake (Figure 3a, zone E, and Figure 4). This suggests that stress release in hypocentral area and its redistribution along the rupture zone has taken a longer time in case of the 1999 Düzce earthquake. Observing the same feature for the recent 2014 Aegean earthquake is not likely due to present temporal limitations. This long-lasting activity is interpreted to represent 10 years of postseismic deformation along the 1999 Düzce rupture zone [*Ergintav et al.,* 2009].

The Sea of Marmara active zones (zones C and D) indicate a generally stable seismicity trend for the entire period of the analysis, expect for a minor response to the 1999 Izmit earthquake. This suggests that the Sea of Marmara segments of the North Anatolian Fault presently accommodate steady, interseismic deformation. However, a large earthquake ($M > 7$) is expected in this region during forthcoming decades based on the occurrence period for the last two destructive events in this particular area, which occurred in 1509 and 1766 [*Parsons*, 2004; *Bohnhoff et al.,* 2013; *Ergintav et al.,* 2014]. Based on the observations before the 1999 and 2014 earthquakes, one of those two zones might potentially accommodate nucleation zone of expected major earthquake.

5. Conclusions

Kandilli Observatory has significantly improved the seismic network in the target area during the last several decades. These improvements began in the immediate vicinity of the Istanbul region and expanded into

other regions in NW Turkey. My analysis indicates that M_c ranges from M 2.5 to M 3.0 in time and space along the western segments of the NAF in NW Turkey. Accordingly, in order to make a robust analysis on a reliable statistical basis of temporal and spatial variations in seismicity, the earthquake catalog I use is restricted to $M > 3.0$.

Hypocentral areas of the 1999 İzmit and the 2014 Aegean earthquakes accommodate long-lasting microearthquake activity during the years leading up to these events. This pattern is clearly different from the rest of target area and therefore is interpreted to represent a characteristic preseismic behavior for those two large earthquakes. In both cases, preshock activity includes sideward migration of microearthquakes toward the main shock hypocenter within a time scale of roughly a decade. In the case of 2014 Aegean earthquake, accelerated activity initiated following the 2003 Saros earthquake and lasted for 11 years. This accelerated activity shows an expanding pattern of seismicity in time and space starting from the 2003 Saros earthquake that migrates toward the 2014 Aegean earthquake.

Aftershock activity in the close vicinity of the main shocks decreased sharply in 2 years in case of the 1999 Izmit earthquake, while it took ~10 years in case of the 1999 Düzce earthquake to return to the background seismicity rate. The 1999 Düzce main shock area did not host long-lasting preshock activity except for the 87 days of the 1999 Izmit aftershocks. Therefore, 1999 Düzce earthquake exemplifies very different preseismic and postseismic stages in terms of seismic activity. This shows that the duration of aftershock activity, and therefore, the postseismic slip is not controlled only by the size of main shocks.

Acknowledgments

The earthquake catalog used in this study is generated by Boğaziçi University, Kandilli Observatory and Earthquake Research Institute, National Earthquake Monitoring Centre. These data are open to public access at the website "http://udim.koeri.boun.edu.tr." I would like to thank A. V. Newman, M. Brehme and T. Taymaz for their constructive comments on the manuscript. Additionally, I would like to thank R. Reilinger for his constructive comments and valuable inputs. Finally, I am grateful to B. Can for her careful readings and corrections.

The Editor thanks Tuncay Taymaz and an anonymous reviewer for their assistance in evaluating this paper.

References

Barka, A. A. (1996), Slip distribution along the North Anatolian fault associated with the large earthquakes of the period 1939 to 1967, *Bull. Seismol. Soc. Am.*, *86*(5), 1238–1254.

Bohnhoff, M., F. Bulut, G. Dresen, P. E. Malin, T. Eken, and M. Aktar (2013), An earthquake gap south of Istanbul, *Nature*, doi:10.1038/ncomms2999.

Bouchon, M., H. Karabulut, M. Aktar, S. Özalaybey, J. Schmittbuhl, and M. P. Bouin (2011), Extended nucleation of the 1999 M_w 7.6 Izmit earthquake, *Science*, *331*, 877–880.

Bulut, F., and M. Aktar (2007), Accurate relocation of Izmit earthquake (M_w = 7.4, 1999) aftershocks in Çinarcik Basin using double difference method, *Geophys. Res. Lett.*, *34*, L10307, doi:10.1029/2007GL029611.

Bürgmann, R., S. Ergintav, P. Segall, E. Hearn, S. McClusky, R. Reilinger, H. Woith, and J. Zschau (2002), Time-dependent distributed afterslip on and deep below the Izmit earthquake rupture, *Bull. Seismol. Soc. Am.*, *92*, 126–137, doi:10.1785/0120000833.

Ergintav, S., S. McClusky, E. H. Hearn, R. E. Reilinger, R. Çakmak, T. Herring, H. Ozener, O. Lenk, and E. Tari (2009), Seven years of postseismic deformation following the 1999, M = 7.4 and M = 7.2, Izmit-Düzce, Turkey earthquake sequence, *J. Geophys. Res.*, *114*, B07403, doi:10.1029/2008JB006021.

Ergintav, S., R. E. Reilinger, R. Çakmak, M. Floyd, Z. Cakir, U. Doğan, R. W. King, S. McClusky, and H. Özener (2014), Istanbul's earthquake hot spots: Geodetic constraints on strain accumulation along faults in the Marmara seismic gap, *Geophys. Res. Lett.*, *41*, 5783–5788, doi:10.1002/2014GL060985.

Evangelidis, C. (2015), Imaging supershear rupture for the 2014 M_w 6.9 Northern Aegean earthquake by backprojection of strong motion waveforms, *Geophys. Res. Lett.*, *42*, 307–315, doi:10.1002/2014GL062513.

Gutenberg, B., and C. F. Richter (1954), Frequency and energy of earthquakes, in *Seismicity of the Earth and Associated Phenomena*, 2nd ed., pp. 17–19, Princeton Univ. Press, Princeton, N. J.

Hanks, T., and H. Kanamori (1979), Moment magnitude scale, *J. Geophys. Res.*, *84*, 2348–2350, doi:10.1029/JB084iB05p02348.

Jackson, J., and D. McKenzie (1988), The relationship between plate motions and seismic moment tensors, and the rates of active deformation in the Mediterranean and Middle East, *Geophys. J.*, *93*, 45–73.

Kalafat, D., et al. (2008), An earthquake catalog for Turkey and the surrounding area ($M \geq$3.0; 1900–2008), Kandilli Observatory and DAE, UDIM, Istanbul (in Turkish).

Karabulut, H., Z. Roumelioti, C. Benetatos, M. Ahu Komec, S. Özalaybey, M. Aktar, and A. Kiratzi (2006), A source study of the 6 July 2003 (M_w 5.7) earthquake sequence in the Gulf of Saros (northern Aegean Sea): Seismological evidence for the western continuation of the Ganos fault, *Tectonophysics*, *412*, 195–216, doi:10.1016/j.tecto.2005.09.009.

King, G. C. P., R. S. Stein, and J. Lin (1994), Static stress changes and the triggering of earthquakes, *Bull. Seismol. Soc. Am.*, *84*(3), 935–953.

Lapusta, N., and J. R. Rice (2003), Nucleation and early seismic propagation of small and large events in a crustal earthquake model, *J. Geophys. Res.*, *108*(B4), 2205, doi:10.1029/2001JB000793.

Meade, B. J., B. H. Hager, S. C. McClusky, R. E. Reilinger, S. Ergintav, O. Lenk, A. Barka, and H. Özener (2002), Estimates of seismic potential in the Marmara Sea region from block models of secular deformation constrained by Global Positioning System measurements, *Bull. Seismol. Soc. Am.*, *92*, 208–215, doi:10.1785/0120000837.

Parsons, T. (2004), Recalculated probability of $M \geq 7$ earthquakes beneath the Sea of Marmara, Turkey, *J. Geophys. Res.*, *109*, B05304, doi:10.1029/2003JB002667.

Reilinger, R. E., et al. (2006), GPS constraints on continental deformation in the Africa-Arabia-Eurasia continental collision zone and implications for the dynamics of plate interactions, *J. Geophys. Res.*, *111*, B05411, doi:10.1029/2005JB004051.

Segall, P., and R. Harris (1987), Earthquake deformation cycle on the San Andreas Fault near Parkfield, California, *J. Geophys. Res.*, *92*, 10,511–10,525, doi:10.1029/JB092iB10p10511.

Şengör, A. M. C., and Y. Yılmaz (1981), Tethyan evolution of Turkey: A plate tectonic approach, *Tectonophysics*, *75*, 181–241.

Şengör, A. M. C., O. Tuysuz, C. Imren, M. Sakinc, H. Eyidogan, G. Görür, X. Le Pichon, and C. Rangin (2005), The North Anatolian Fault: A new look, *Annu. Rev. Earth Planet. Sci.*, *33*, 37–112, doi:10.1146/annurev.earth.32.101802.120415.

Taymaz, T., J. A. Jackson, and R. Westaway (1990), Earthquake mechanisms in the Hellenic Trench near Crete, *Geophys. J. Int.*, *102*, 695–731.

Taymaz, T., J. A. Jackson, and D. McKenzie (1991), Active tectonics of the North and Central Aegean Sea, *Geophys. J. Int.*, *106*, 433–490.
Toksöz, M. N., A. F. Shakal, and A. J. Michael (1979), Space-time migration of earthquakes along the North Anatolian Fault zone and seismic gaps, *Pure Appl. Geophys.*, *117*, 1258–1270.
Yolsal-Çevikbilen, S., and T. Taymaz (2012), Earthquake source parameters along the Hellenic subduction zone and numerical simulations of historical tsunamis in the Eastern Mediterranean, *Tectonophysics*, *536–537*, 61–100.